NACA

RESEARCH MEMORANDUM

INVESTIGATION OF A 0.6 HUB-TIP RADIUS-RATIO TRANSONIC TURBINE DESIGNED FOR SECONDARY-FLOW STUDY

III - EXPERIMENTAL PERFORMANCE WITH TWO STATOR CONFIGURATIONS DESIGNED TO ELIMINATE BLADE WAKES AND SECONDARY-FLOW EFFECTS AND CONCLUSIONS FROM ENTIRE STATOR INVESTIGATION

By Harold E. Rohlik, William T. Wintucky, and Thomas P. Moffitt

Lewis Flight Propulsion Laboratory
Cleveland, Ohio

NATIONAL ADVISORY COMMITTEE
FOR AERONAUTICS

WASHINGTON

September 17, 1957

NATIONAL ADVISORY COMMITTEE FOR AERONAUTICS

RESEARCH MEMORANDUM

INVESTIGATION OF A 0.6 HUB-TIP RADIUS-RATIO TRANSONIC TURBINE DESIGNED FOR SECONDARY-FLOW STUDY

III - EXPERIMENTAL PERFORMANCE WITH TWO STATOR CONFIGURATIONS DESIGNED TO ELIMINATE BLADE WAKES AND SECONDARY-FLOW EFFECTS AND CONCLUSIONS FROM ENTIRE STATOR INVESTIGATION

By Harold E. Rohlik, William T. Wintucky, and Thomas P. Moffitt

SUMMARY

Two turbine stator configurations were designed in order to investigate the effect on turbine performance of either reducing or eliminating stator-blade wakes, secondary-flow loss accumulations, and circumferential variations in total pressure at the stator exits. One configuration, the semivaneless stator, consisted of a blade row that turned the air at flow radii greater than those at the rotor entrance and, therefore, at lower velocities, and then accelerated it in a vaneless passage of decreasing radii. The other configuration provided a vaneless annular passage between the stator and the rotor comparable in length to the vaneless section of the semivaneless stator. Both stators were tested with the rotor of the standard turbine previously investigated and reported, and results are compared herein with those obtained with the standard turbine.

The semivaneless stator caused poor rotor performance in that the turbine produced only 96.5 percent of design work at design speed with a turbine total efficiency of 0.815, compared with 0.863 obtained with the same rotor and the standard stator.

Rotor performance obtained with the standard stator with spacer was better than that obtained with the standard configuration. This improvement apparently resulted from the fact that, with this spacer, the stator-blade-wake mixing losses were incurred upstream of the rotor while, in the standard configuration, some mixing occurred in the rotor and therefore was measured as a rotor loss. Design specific work was obtained at design speed with an efficiency of 0.847.

The investigation of stator secondary flows showed that stator-blade wakes and secondary-flow accumulations can be effectively and efficiently eliminated.

No configuration studied in the stator investigation improved the over-all performance previously obtained with the standard stator located immediately upstream of the rotor. This lack of improvement is believed to be caused partly by near-critical rotor-blade loading that made the blade boundary layers subject to separation with small changes in loss distribution and turbulence level.

INTRODUCTION

An investigation of the effects of stator and rotor secondary flows on over-all performance of a transonic turbine is being conducted at the NACA Lewis laboratory. Evaluation of these effects is being made by studying the changes in over-all performance and internal-flow conditions that result from modification of secondary-flow patterns. Reference 1 presents the design and over-all performance of the standard turbine, as well as a detailed picture of internal-flow conditions at design-point operation of the turbine.

Two turbine-stator configurations were designed in order to investigate the effect on turbine performance of reducing the circumferential variations in velocity. A semivaneless stator was designed to turn the air in a blade row to design moment of momentum at hub and tip radii greater than the rotor hub and tip radii and at relatively low velocities. Acceleration to design rotor-inlet conditions is then completed in a vaneless section that mixes the wakes and secondary-flow loss accumulations which developed in the blade row at low-energy levels. Detailed information on the design method and analysis of flow conditions in the vaneless part of this stator is given in reference 2. The other stator configuration consisted of a conventional stator-blade row followed by a vaneless annular spacer approximately equal in length to the vaneless part of the semivaneless stator; this stator permitted mixing at design stator-exit kinetic-energy levels.

The primary purpose of the present report is to give in detail the rotor-inlet flow conditions caused by each of the two stators and the turbine performance with each stator. Turbine performance is presented in terms of specific work, weight flow, and efficiency over a wide range of speed and pressure ratios, as well as the local efficiency distribution at the rotor exit obtained at design speed near design work. These results are compared with information obtained in a similar investigation with the standard stator and the same rotor (ref. 1). The secondary purpose of this report is to present the major conclusions drawn from the entire stator secondary-flow investigation.

SYMBOLS

Δh specific enthalpy drop, Btu/lb

l mean camber length, ft

N rotative speed, rpm

p absolute gas pressure, lb/sq ft

r radius, ft

U blade velocity, ft/sec

V absolute gas velocity, ft/sec

W relative gas velocity, ft/sec

w weight flow, lb/sec

α absolute gas-flow angle measured from axial direction, deg

β relative gas-flow angle measured from axial direction, deg

γ ratio of specific heats

δ ratio of inlet-air total pressure to NACA standard sea-level pressure of 2116 lb/sq ft

ε function of $\gamma, \frac{\gamma_{sl}}{\gamma}\left[\frac{\left(\frac{\gamma+1}{2}\right)^{\frac{\gamma}{\gamma-1}}}{\left(\frac{\gamma_{sl}+1}{2}\right)^{\frac{\gamma_{sl}}{\gamma_{sl}-1}}}\right]$

η total efficiency; ratio of turbine work based on torque, weight flow, and speed measurements to ideal work based on inlet total temperature, and inlet and outlet total pressure, both defined as sum of static pressure plus pressure corresponding to gas velocity calculated from flow area and continuity

η_x rating efficiency; ratio of turbine work based on torque, weight flow, and speed measurements to ideal work based on inlet total temperature, and inlet and outlet total pressure, both defined as sum of static pressure plus pressure corresponding to calculated average axial component of velocity

θ_{cr} squared ratio of critical velocity at turbine inlet to critical velocity at NACA standard sea-level temperature $V_{cr}/V_{cr,sl}$

$\overline{\theta}$ effective rotor-blade momentum thickness based on turbine over-all performance, ft

θ^* momentum-loss parameter defined as ratio of total momentum thickness to blade spacing

Subscripts:

cr conditions at Mach number of 1.0

sl NACA standard sea-level conditions

t tip

u tangential direction

x axial direction

0 station upstream of stator

1 station at throat of stator passage

2 station at outlet of stator just upstream of trailing edge

2a station at outlet of semivaneless stator-blade row

3 station at free-stream condition at rotor inlet

4 station at throat of rotor passage

5 station at outlet of rotor just upstream of trailing edge

6 station downstream of turbine

Superscript:

' absolute total state

APPARATUS, INSTRUMENTATION, AND PROCEDURE

The test apparatus and the method of calculating the stator and turbine performance parameters are the same as those used in reference 1. Reference 2 describes in detail the design and performance of the semivaneless stator. The three stator configurations discussed in this

report (including the standard stator previously reported in ref. 1) were designed to produce the station-3 velocity diagrams shown in figure 1. The blade row of the semivaneless stator was designed for the station 2(a) velocity diagrams also shown in figure 1. The semivaneless stator and the standard stator with spacer are diagramatically shown in figures 2 and 3, respectively. Two concentric cylindrical spacers were installed between the standard stator and the rotor to provide a constant annular area at constant hub and tip radii and a flow path approximately equal in length to that of the transition section of the semivaneless stator.

The method of turbine operation used to obtain over-all performance and annular surveys was the same as that used in reference 1. Surveys were made at stator and rotor exits (stations 3 and 6, figs. 2 and 3) with the rotor operating at design speed and near design work.

RESULTS AND DISCUSSION

Stator Surveys

Results of annular surveys of total pressure made at the stator exit were used to prepare contours of total-pressure ratio for each stator configuration.

The contours for the semivaneless stator (fig. 4(a)) show almost complete mixing with traces of the blade wakes in, and close to, the outer-wall boundary layer only. The calculated total-pressure ratio corresponding to these contours was 0.973, which indicates that this method of stator-blade loss control provided efficient mixing during the acceleration in the vaneless part of the stator.

The contours of figure 4(b) show the loss pattern at station 3 with the standard stator with spacer. This stator, which mixes the blade wakes and secondary-flow accumulations at the high kinetic-energy levels corresponding to the velocity diagrams shown in figure 1, provides complete mixing in the inner half of the annulus and considerable mixing in the outer half. The wakes and loss cores in the outer half of the passage are clearly defined, but the maximum loss in the cores is about 0.08, compared with 0.16 immediately behind the blades, as shown in figure 4(c), which is taken from reference 1. Losses developed in mixing at this energy level were much larger than in the semivaneless stator. The over-all total-pressure ratio for this configuration was 0.946.

Figure 4(c) shows contours of total-pressure ratio obtained from surveys made about 3/4 inch downstream of the standard stator-blade trailing edges for comparison with figures 4(a) and (b). The blade wakes and secondary-flow accumulations are clearly defined, and the total-pressure ratio for this stator was 0.975.

Figure 5 shows the radial distribution of the momentum-loss parameter θ^* for the standard stator, the semivaneless stator, and the standard stator with spacer. The momentum-loss distributions for the standard and the semivaneless stators are comparable, with slight local variations in level and with a thicker inner-wall boundary layer indicated for the semivaneless stator. The standard stator with spacer, however, resulted in greater momentum losses at all radii, with thicker boundary layers indicated on both inner and outer walls.

Stator-exit surveys of total pressure and flow angle were used with static pressures obtained from a radial curve faired between wall static-pressure measurements to compute the radial distribution of moment of momentum for the two stator configurations described in this report, in order to evaluate stator performance in terms of work potential for the rotor. Figure 6 shows that both stators performed satisfactorily in this respect with slightly more than design moment of momentum in most of the free stream and with less in the wall boundary layers.

Relative flow angles were calculated by using static pressures read from the curve faired between wall measurements and measured values at total pressure, absolute flow angle, and wheel speed.

Figure 7 shows design and experimental radial distributions of relative flow angle for the semivaneless stator and the standard stator with spacer and indicates very small incidence angles in all but the wall boundary layers.

Figures 6 and 7 show that both stators performed satisfactorily in setting up design flow conditions for the rotor. The moment of momentum is uniformly distributed from hub to tip at a level slightly above the design value, and the angle distribution indicates good incidence characteristics.

Over-all Performance with Semivaneless Stator

Performance maps based on total-pressure and rating pressure ratios are shown in figure 8 for turbine operation with the semivaneless stator. Maximum work obtained at design speed was only 20.95 Btu per pound, 3.5 percent below the design value of 21.70 Btu per pound. Turbine efficiencies in the high speed - high work part of the maps were considerably lower than the efficiencies obtained with the standard stator of reference 1.

Maximum total efficiency obtained with the semivaneless stator was 0.823 and occurred at 110 percent design speed near limiting work. Maximum rating efficiency was 0.822 and also occurred at 110 percent design speed near limiting work. Design-point total efficiency for the standard

configuration of reference 1 was 0.863, while the total efficiency obtained with the semivaneless stator was 0.815 at design speed near limiting work. Comparison of figures 8(a) and (b) indicates a very small loss in rating efficiency due to exit whirl, as was also the case with the reference turbine.

The difference in total-pressure ratio between the standard stator of reference 1 and the semivaneless stator was 0.002, which would result in a difference of 0.002 in turbine efficiency at design work if rotor performance remained unchanged. The measured difference in efficiency near design work, however, was 0.048. It is apparent that rotor-blade performance was considerably poorer when operated behind the semivaneless stator rather than the standard stator. Angle measurements made at the rotor exit during performance tests confirmed this by showing a radial variation of 15° in absolute flow angle with a positive value at the midspan of 5.9°, compared with the design value of -5.1°. This variation, when converted to relative flow angles with measured air velocity and wheel speed, means that the rotor turned the air 10.2° less than design turning at the blade midspan.

Underturning near the rotor-blade midspan was experienced to a lesser degree with the standard stator and is discussed in reference 1. This underturning apparently is the result of rotor-blade boundary-layer behavior. The same type of boundary-layer behavior was encountered in the investigation of reference 3 and is discussed in detail therein. In brief, the rotor blade of reference 3 was designed for relatively high-pressure surface diffusion, as was the rotor of this investigation; this design could result in a thickening of the boundary layer on the pressure surface near the leading edge and thus provide a path for blade boundary-layer flow toward the hub, because the radial pressure force associated with the high level of whirl would predominate over centrifugal forces. The accumulation of low-velocity material at the rotor hub, resulting from rotor secondary flows and the stator inner-wall boundary layer, would then flow radially outward in the blade boundary layers near the trailing edge, where centrifugal forces would predominate over pressure forces because of the reduced whirl. It was further theorized in reference 3 that the net effect of these flows would be an accumulation of loss material near the blade midspan at the rotor exit. The underturning, then, apparently results from poor rotor-blade element performance at the midspan induced by the thickened boundary layers, which might cause separation and consequently less-than-design loading.

The difference in limiting work between the standard turbine and the turbine with the semivaneless stator results directly from a loss of turning at the rotor midspan, which in turn is related to rotor-blade boundary-layer behavior and is not the result of a lack of circumferential momentum at the stator exit or rotor incidence angles. The deterioration in rotor-blade performance appears to result from a lower turbulence level with the semivaneless stator, which consequently means a greater likelihood of separation and loss of blade loading. The turbulence level

at the semivaneless stator exit was lower than at the exit of the standard stator because of the lower kinetic-energy level in the vicinity of the blades, where the random velocities contributing to turbulence originate. Acceleration in the vaneless part is accomplished without local disturbances in flow, so that turbulent energy would constitute a smaller fraction of the total kinetic energy at the stator exit than it would with the standard stator, where the blades support large velocity gradients at the higher energy levels. The rotor blade used in this investigation was designed for relatively high loading and high blade surface diffusion, as described in reference 1. Because of this high diffusion, the boundary layer appears to be somewhat unstable and is likely to separate as a result of only slight changes in turbulence level. A rotor designed for more conservative blade loading might not respond to the difference in turbulence.

Over-all Performance with the Standard Stator with Spacer

Turbine performance maps based on total-pressure and rating pressure ratios are shown in figure 9. Limiting work at design speed is slightly above design work and is approximately equal to the limiting work measured with the standard configuration of reference 1. Weight flow obtained with this configuration at design speed and work was 1 percent lower than that obtained with the standard stator of reference 1. This difference partly offset the increase in equivalent flow at the stator exit caused by the mixing losses and permitted the stator to produce a near-design value of whirl before the rotor choked at this speed. Maximum total efficiency obtained with the standard stator with spacer was 0.862 and occurred at 120 percent design speed near limiting work. Maximum rating efficiency was 0.861 and occurred at about 115 percent design speed. Total efficiency at design-point operation was 0.847, compared with 0.863 obtained without the spacer. This difference of 0.016 is less than the loss in turbine efficiency caused by mixing loss between the stator- and rotor-blade rows and would result in a turbine loss of 0.028 at design work if rotor pressure loss remained constant. This apparent improvement in rotor performance is probably the result of the uniform flow at the rotor inlet, which eliminates stator-blade-wake mixing from the rotor passages and therefore results in the measurement of these losses entirely as stator loss rather than rotor loss. Most important, however, is the fact that the rotor operated considerably more efficiently with the standard stator and spacer than with the semivaneless stator at design speed, with a rotor-entrance flow distribution that was approximately the same as that produced by the semivaneless stator. The difference in rotor-blade performance obtained with the two stators apparently results from a difference in turbulence level at the rotor inlet, with a higher turbulence level occurring at the exit of the standard stator with spacer.

Figure 10 shows the radial distribution of rotor-exit absolute flow angle for turbine operation both with the semivaneless stator and with the standard stator with spacer and illustrates the difference in rotor performance in the middle part of the blade. A calculation relating turbine work and exit whirl at design rotor-inlet conditions, made in order to check the differences in exit flow angle shown in figure 10, showed that a loss in turbine work of 3.5 percent (the measured difference in limiting work at design speed between the configurations compared in fig. 10) corresponds to a difference in exit flow angle of 2.6°. The differences shown in figure 10 are of this magnitude.

Rotor-Exit Surveys

Results of rotor-exit surveys were used to obtain the radial distribution of local total turbine efficiency; this is shown in figure 11 for the standard stator, the semivaneless stator, and the standard stator with spacer. All three stators produce similar local efficiency distributions in that highest efficiencies occur near the end walls, while a region of low efficiency occurs in the region of the mean section. The standard stator with and without the spacer results in very similar patterns of efficiency distribution, with a minimum efficiency in the middle part of the passage near 0.82 in both cases. The corresponding efficiency obtained with the semivaneless stator was only 0.77, which confirms the previously noted deterioration in rotor-blade performance near the midspan.

The efficiency levels shown in figure 11 are somewhat higher than efficiencies determined with over-all performance measurements because of the fact that the rotor-exit survey measurements were made in a field of pulsating flow with a frequency set by the wheel speed and number of blades in the rotor. Pressure measurements of this kind result in an indicated pressure that differs from the time average value to a degree and in a direction depending on such variables as probe geometry, wave shape of the pulsations, pressure level, and Reynolds number. The curves presented in figure 11 are considered adequate for comparison purposes, however, because they all were obtained from measurements made at the same frequency and with the same instruments.

Rotor-Blade Momentum Loss

The total-pressure ratios across the three stator configurations and the measured turbine efficiencies at design speed near design work were used with turbine-geometry parameters to obtain values of the ratio of rotor-blade effective-momentum thickness to blade mean camber length. This parameter, described in reference 4, is an index of rotor performance. The calculated values were 0.0152, 0.0226, and 0.0143 for the standard

stator, semivaneless stator, and standard stator with spacer, respectively. The apparent improvement in rotor-blade performance obtained by placing the spacer between the standard stator and the rotor, and therefore completing stator-blade wake mixing upstream of the rotor, is shown here as a 6-percent decrease in momentum thickness. The momentum thickness obtained with the semivaneless stator was 18.5 percent higher than that for the standard configuration of reference 1 and 26 percent higher than for the standard stator with spacer.

The difference in turbine performance among the three stator-rotor combinations described herein and the conclusions reached are believed to be valid because the same instruments and test facility were used to obtain all data. In addition to this, the principal effect of rotor-blade underturning was observed by two independent measurements: (1) total-temperature surveys, which showed different turbine temperature drops at the blade midspan; and (2) absolute flow angle surveys, which showed a large angle variation with minimum turning at the blade midspan where less turning existed with the semivaneless stator than with the standard stator with spacer.

SUMMARY OF RESULTS

An experimental investigation of stator performance and over-all turbine performance was conducted for two turbine configurations: one using a semivaneless stator, and the other using a standard stator with a spacer between the stator and the rotor. Results of the investigation may be summarized as follows:

1. Both stators performed satisfactorily in setting up design moment of momentum and relative inlet flow angle to the rotor. Surveys at the stator exit in both cases indicated nearly complete mixing of stator-blade wakes, thick inner-wall boundary layers, and circumferential uniformity in total-pressure distribution.

2. The maximum work obtainable at design speed from the turbine with the semivaneless stator was only 96.5 percent of design work. This limit occurred because of poor rotor performance near the blade midspan, which turned the flow 10.2° less than design. The total efficiency at this point was 0.815, compared with 0.863 for the standard turbine of reference 1 operating at design work and speed. The maximum total efficiency obtained was 0.823 and occurred at 110 percent design speed near limiting work. This drop in efficiency (0.048) apparently resulted from a pronounced effect on rotor-blade boundary-layer behavior. Mixing at the stator exit occurred at a relatively low kinetic-energy level, and hence the turbulence level was low at the rotor inlet.

3. Design work at design speed was obtained with the standard stator with spacer at slightly less than limiting work. This result was possible

because the stator throat area was somewhat lower than that of the standard configuration; therefore the stator could produce design whirl at design speed before rotor choking, despite the increase in equivalent flow induced by the stator mixing losses. Total efficiency at the design point was 0.847, compared with 0.863 for the standard stator without spacer (ref. 1). This 0.016 decrease in efficiency is less than the decrease that would result from the increased stator losses if rotor performance remained the same. The apparent improvement in rotor performance is explained by the fact that stator-blade wakes are completely mixed upstream of the rotor and consequently do not contribute mixing losses in the rotor.

4. A plot of radial variation in local total efficiency at the rotor exit showed that all three stators produced similar patterns in that a region of low efficiencies occurred at the mean height, with a minimum of about 0.82 for the standard stator with and without the spacer, and 0.77 for the semivaneless stator.

CONCLUDING REMARKS

The investigation of stator secondary flows and their effect on turbine performance has resulted in two major conclusions:

1. The conventional turbine stator-exit loss pattern of blade wakes, wall boundary layers, and secondary-flow loss cores can be efficiently modified as in the semivaneless stator to a pattern of circumferential uniformity in flow angle and velocity. This can be accomplished while establishing a prescribed radial distribution of these parameters with deviations only in the wall boundary layers.

2. Three stator configurations were designed to modify the conventional stator-exit loss pattern: one to reduce only the secondary-flow loss cores, and the other two to mix the stator-blade wakes and the loss cores. None of these configurations resulted in an improvement in overall turbine performance although, with each one, reasonable success was obtained in achieving particular objectives regarding the stator losses. This leads to the conclusion that a conventional stator, with its characteristic exit loss pattern, is the most desirable of the types investigated. This conclusion must be qualified, however, since the rotor used to evaluate the stators was designed for near-critical blade loading and surface diffusion. It is quite possible that a rotor designed for conservative loading and low diffusion would operate more efficiently with a semivaneless stator than with a conventional stator-blade row located immediately upstream of the rotor.

Lewis Flight Propulsion Laboratory
National Advisory Committee for Aeronautics
Cleveland, Ohio, July 9, 1957

REFERENCES

1. Rohlik, Harold E., Wintucky, William T., and Scibbe, Herbert W.: Investigation of a 0.6 Hub-Tip Radius-Ratio Transonic Turbine Designed for Secondary-Flow Study. I - Design and Experimental Performance of Standard Turbine. NACA RM E56J16, 1957.

2. Rohlik, Harold E., and Wintucky, William T.: Investigation of a Semivaneless Turbine Stator Designed to Produce Axially Symmetrical Free-Vortex Flow. NACA TN 3980, 1957.

3. Wong, Robert Y., Miser, James W., and Stewart, Warner L.: Qualitative Study of Flow Characteristics Through Single-Stage Turbines as Made from Rotor-Exit Surveys. NACA RM E55K21, 1956.

4. Stewart, Warner L., Whitney, Warren J., and Miser, James W.: Use of Effective Momentum Thickness in Describing Turbine Rotor-Blade Losses. NACA RM E56B29, 1956.

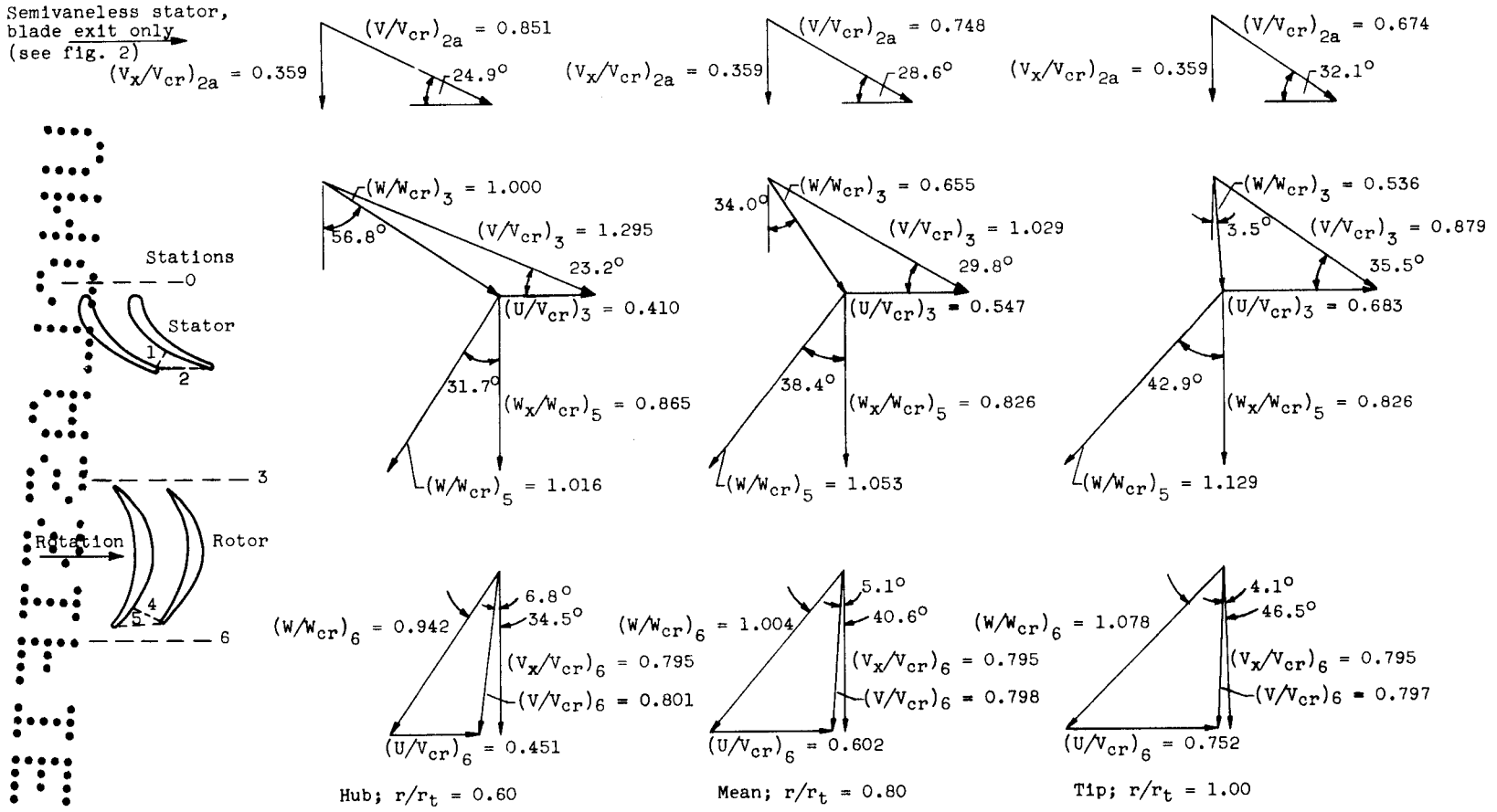

Figure 1. - Design velocity diagrams of transonic secondary-flow turbine.

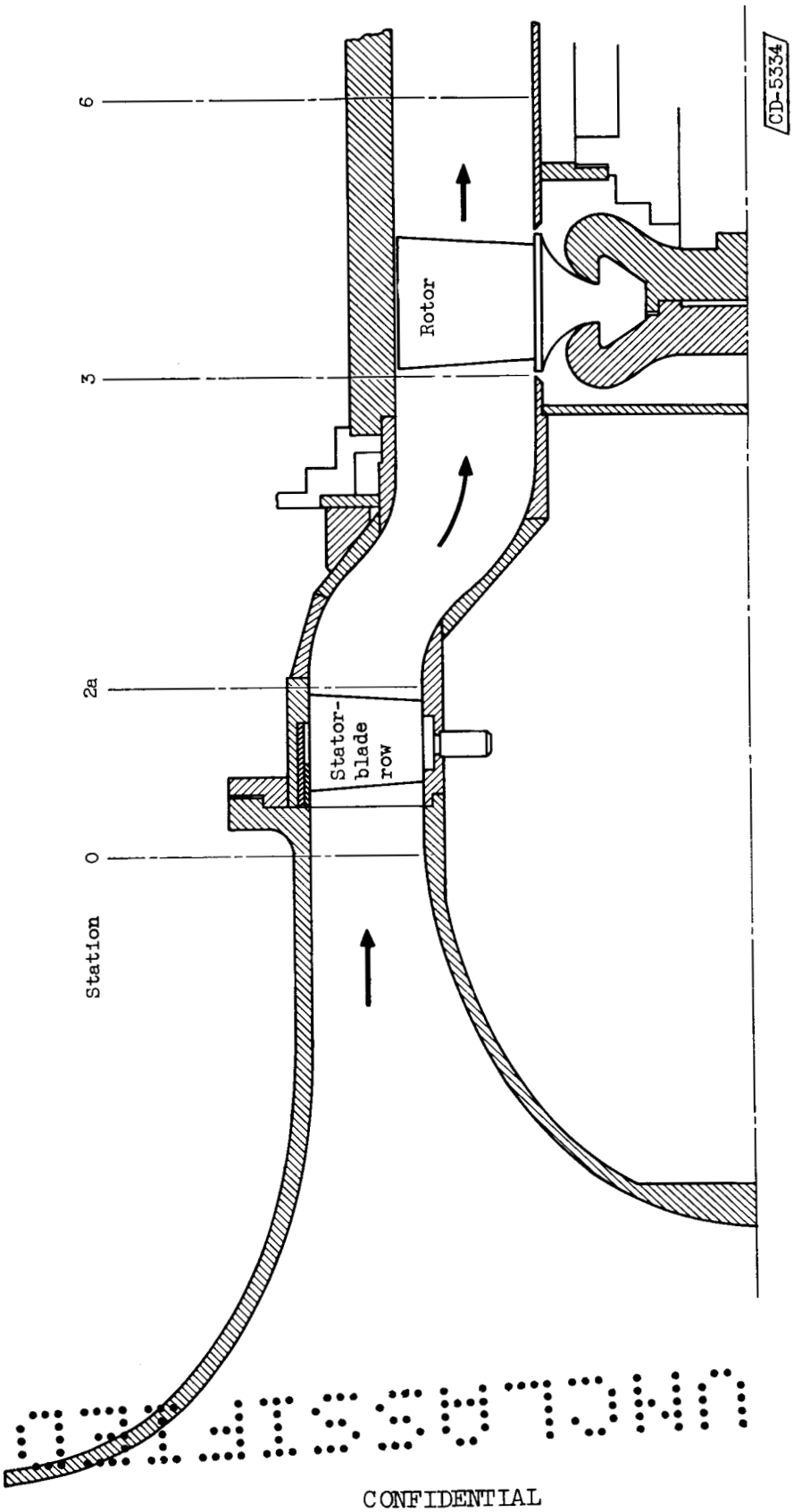

Figure 2. - Turbine with semivaneless stator.

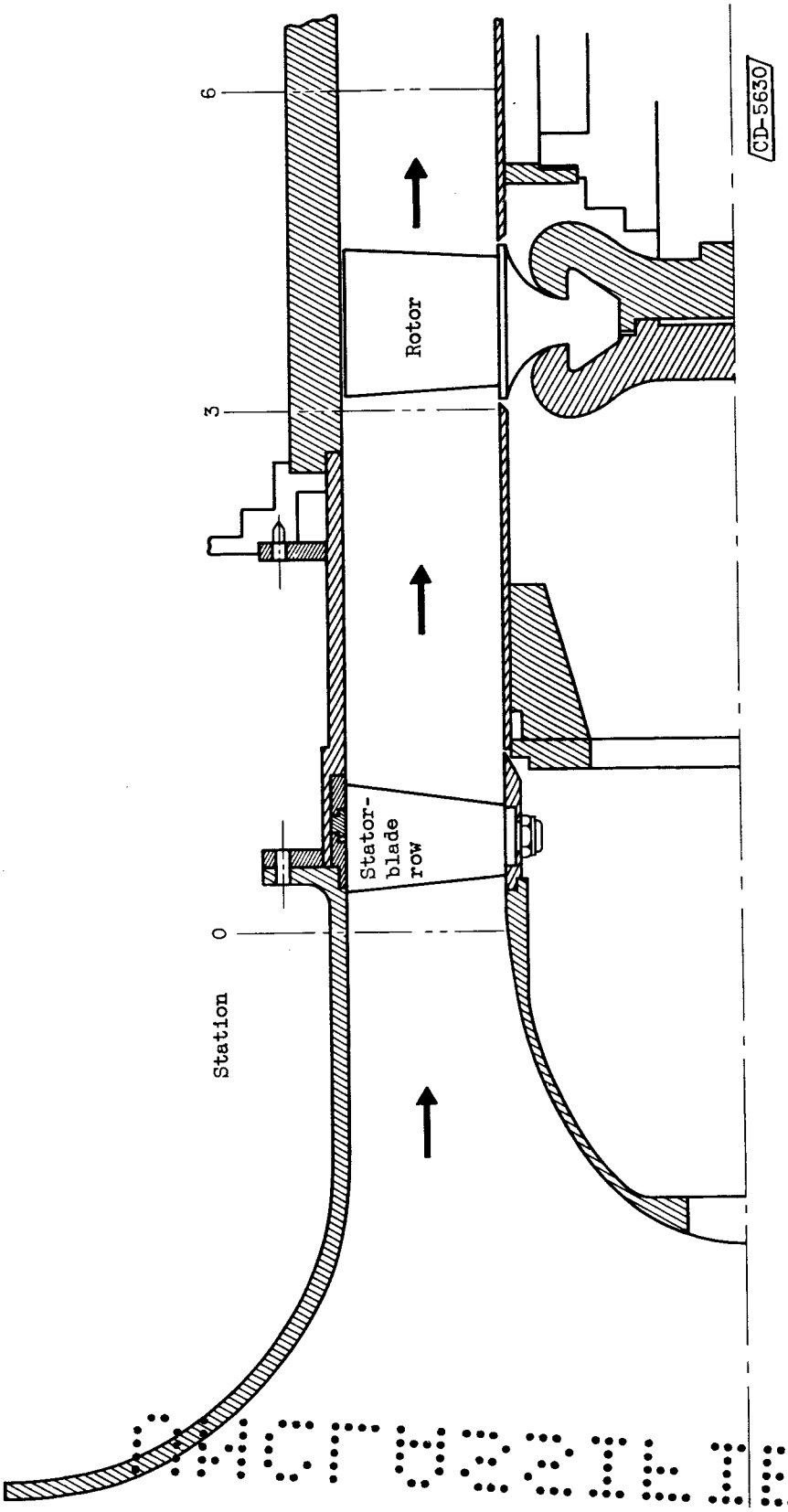

Figure 3. - Turbine with standard stator and spacer.

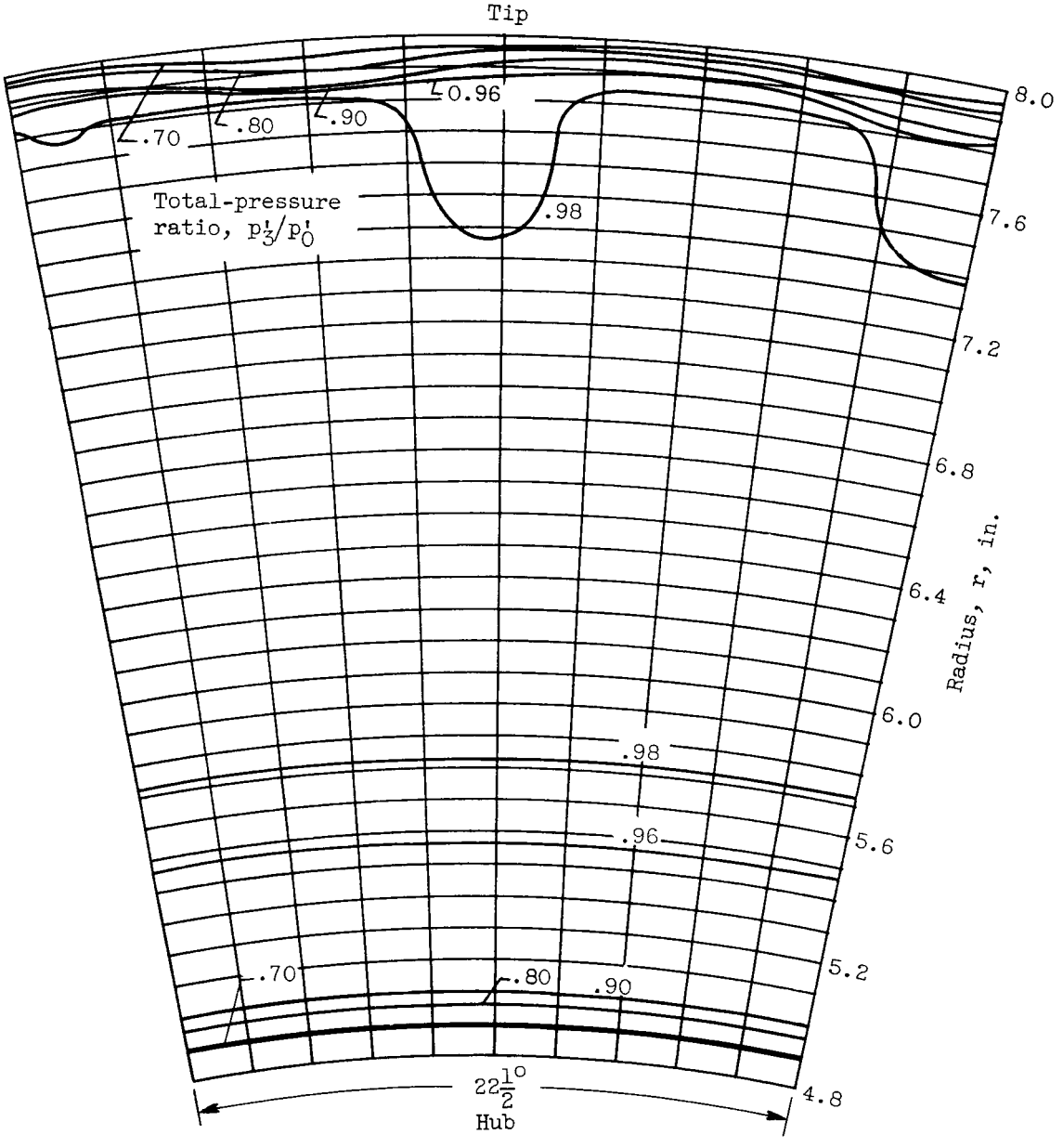

(a) Semivaneless stator.

Figure 4. - Contours of total-pressure ratio at exit measuring station.

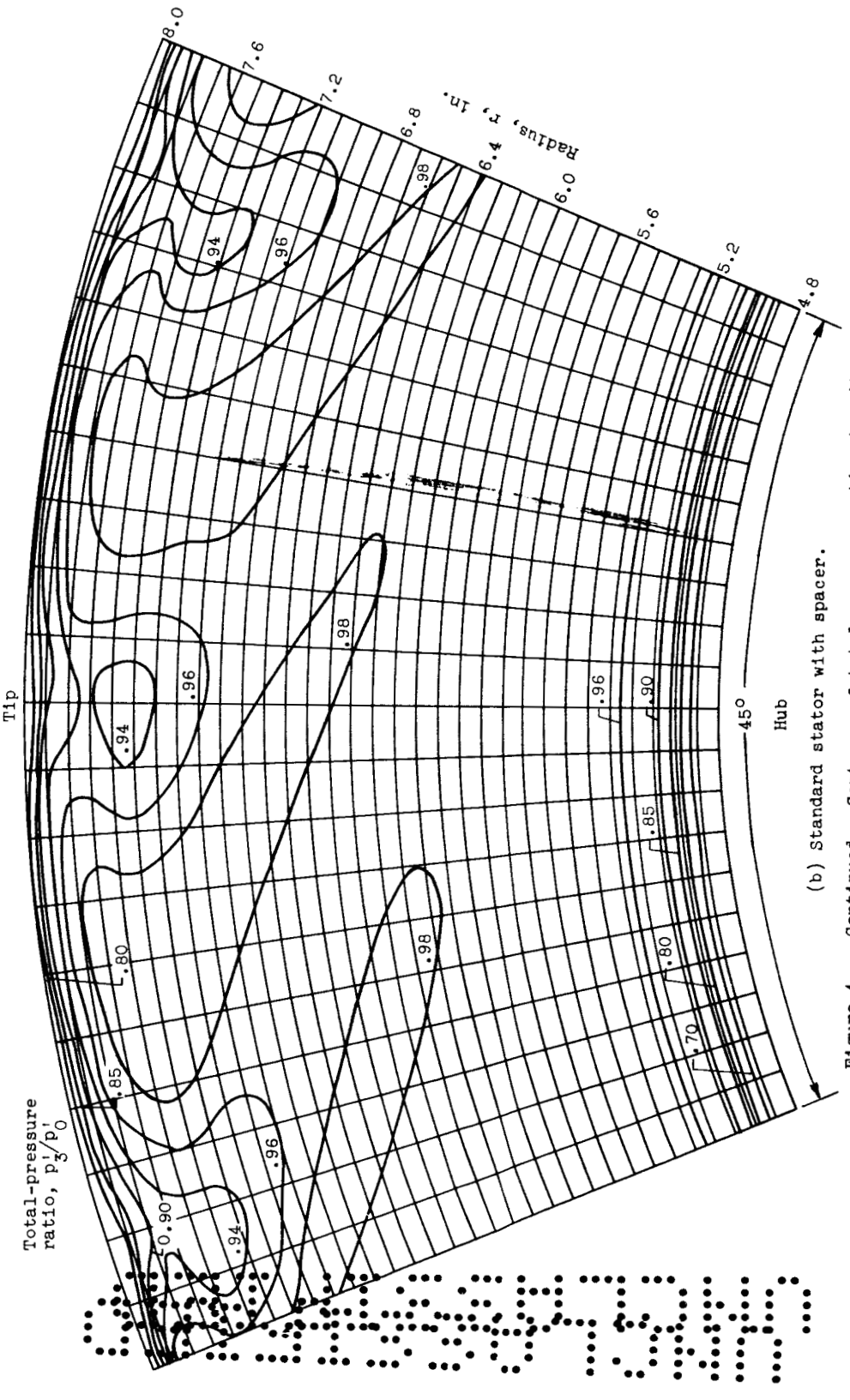

(b) Standard stator with spacer.

Figure 4. - Continued. Contours of total-pressure ratio at exit measuring station.

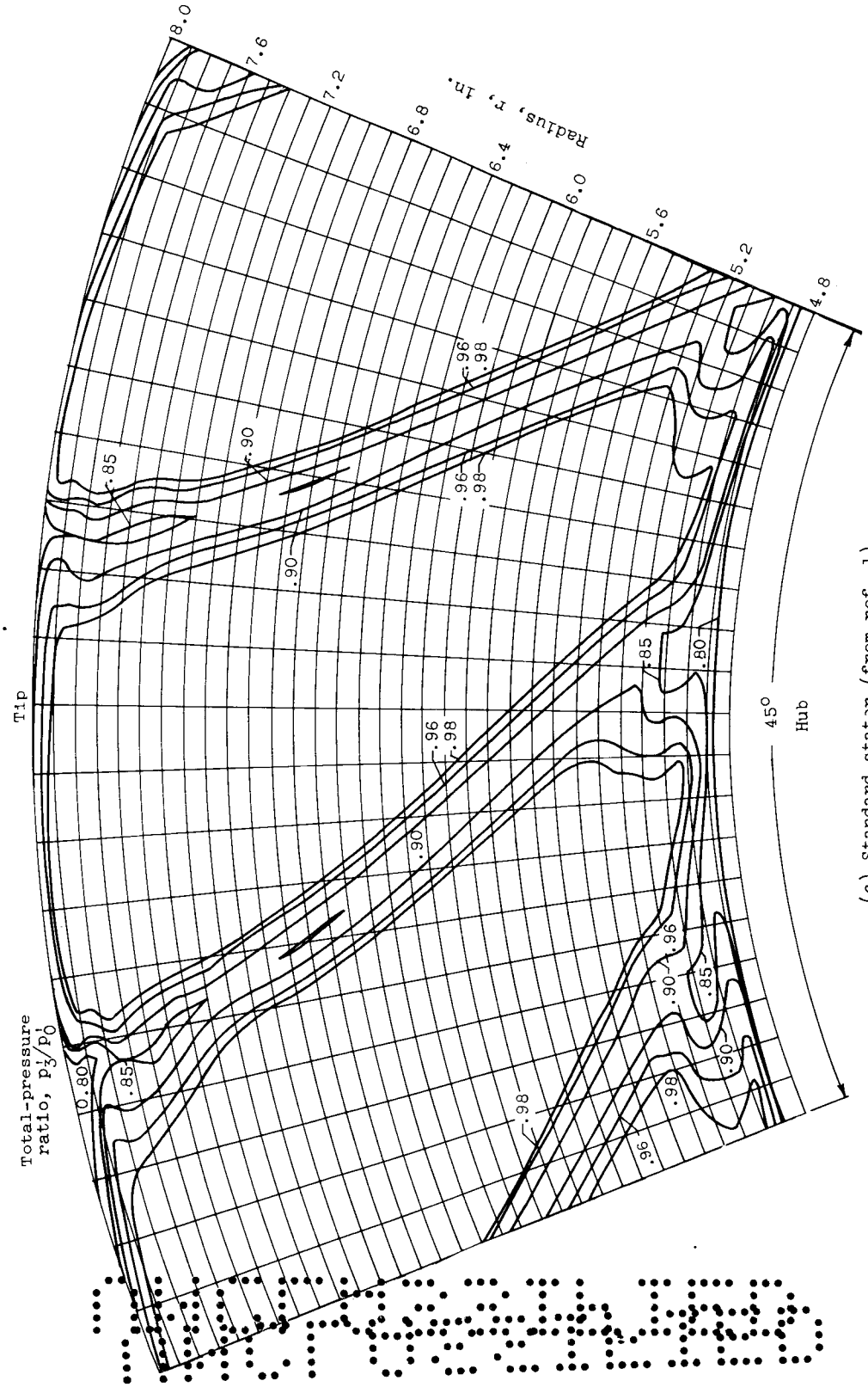

(c) Standard stator (from ref. 1).

Figure 4. - Concluded. Contours of total-pressure ratio at exit measuring station.

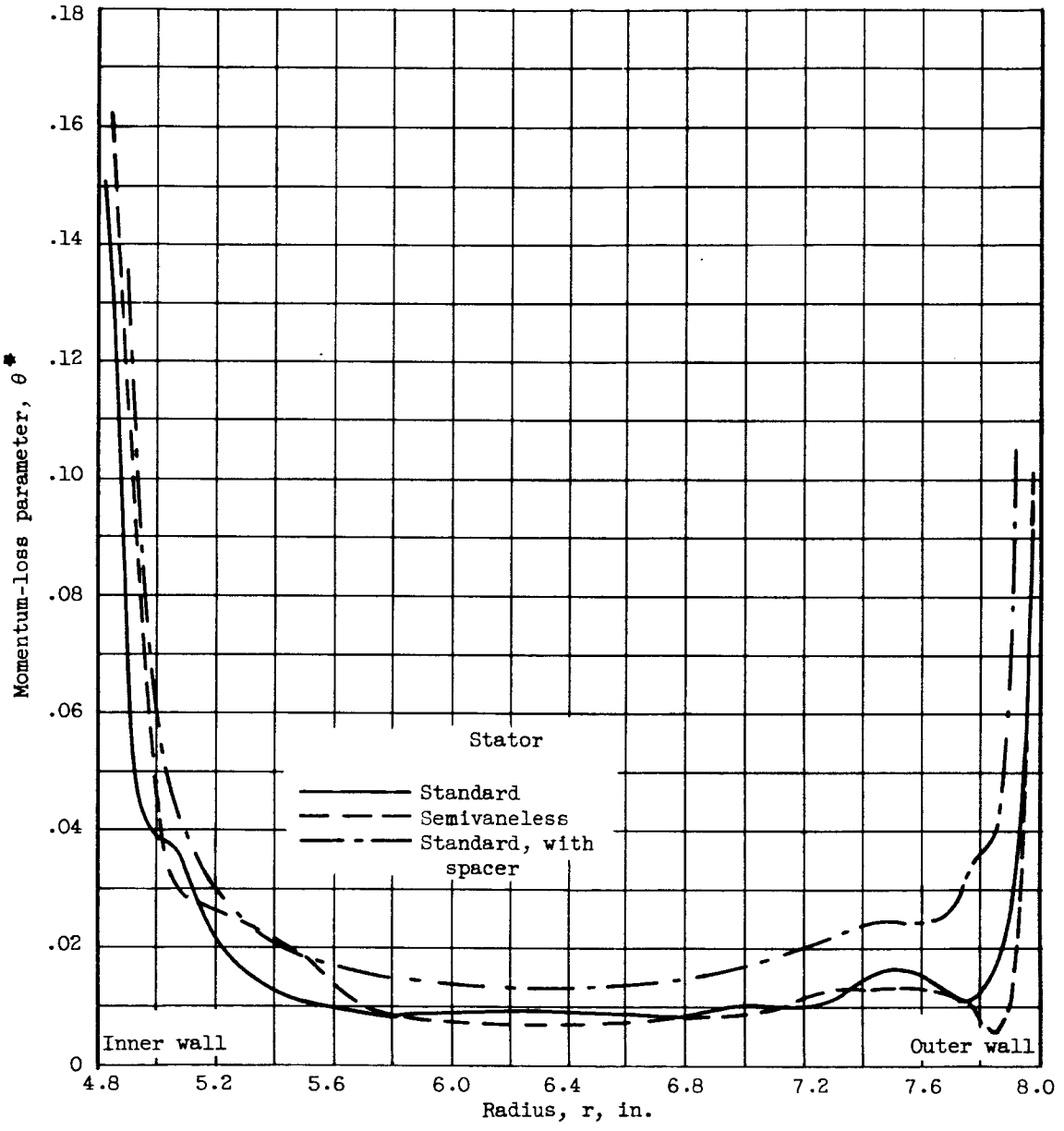

Figure 5. - Radial distribution of momentum-loss parameter at stator-exit survey station.

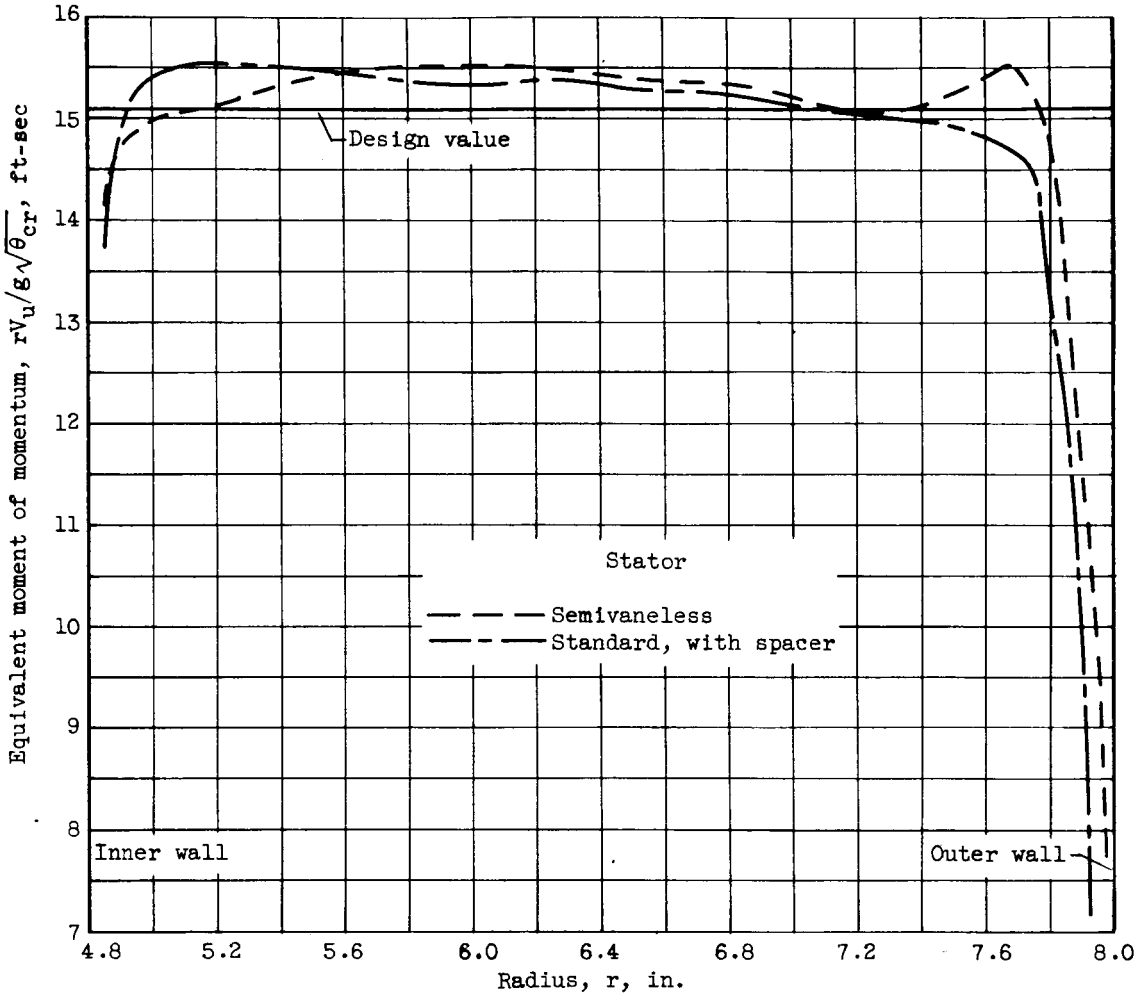

Figure 6. - Radial variation of moment of momentum at rotor entrance with turbine operating at design speed near limiting work.

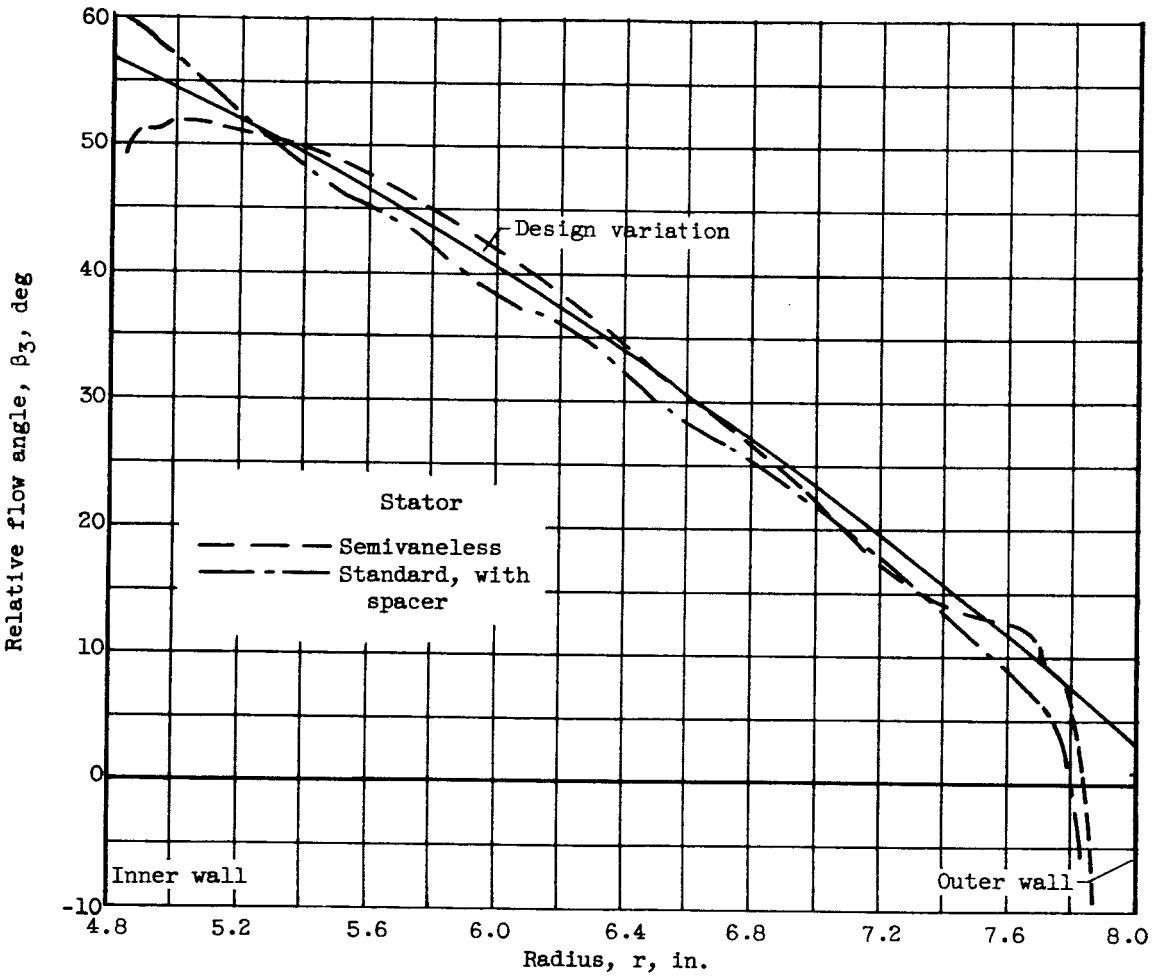

Figure 7. - Radial variation in relative flow angle at rotor inlet.

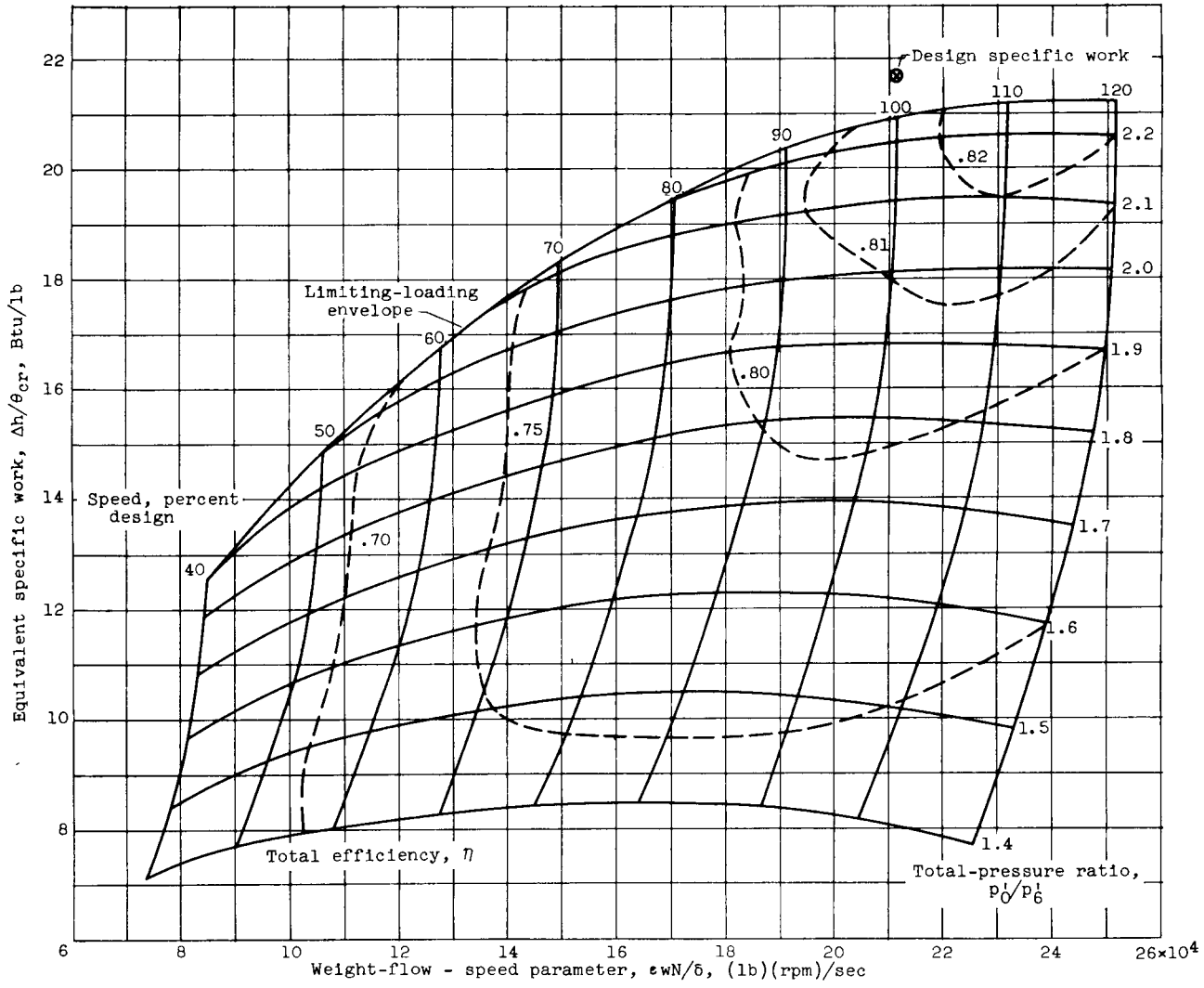

(a) Based on total-pressure ratio.

Figure 8. - Over-all turbine performance with semivaneless stator.

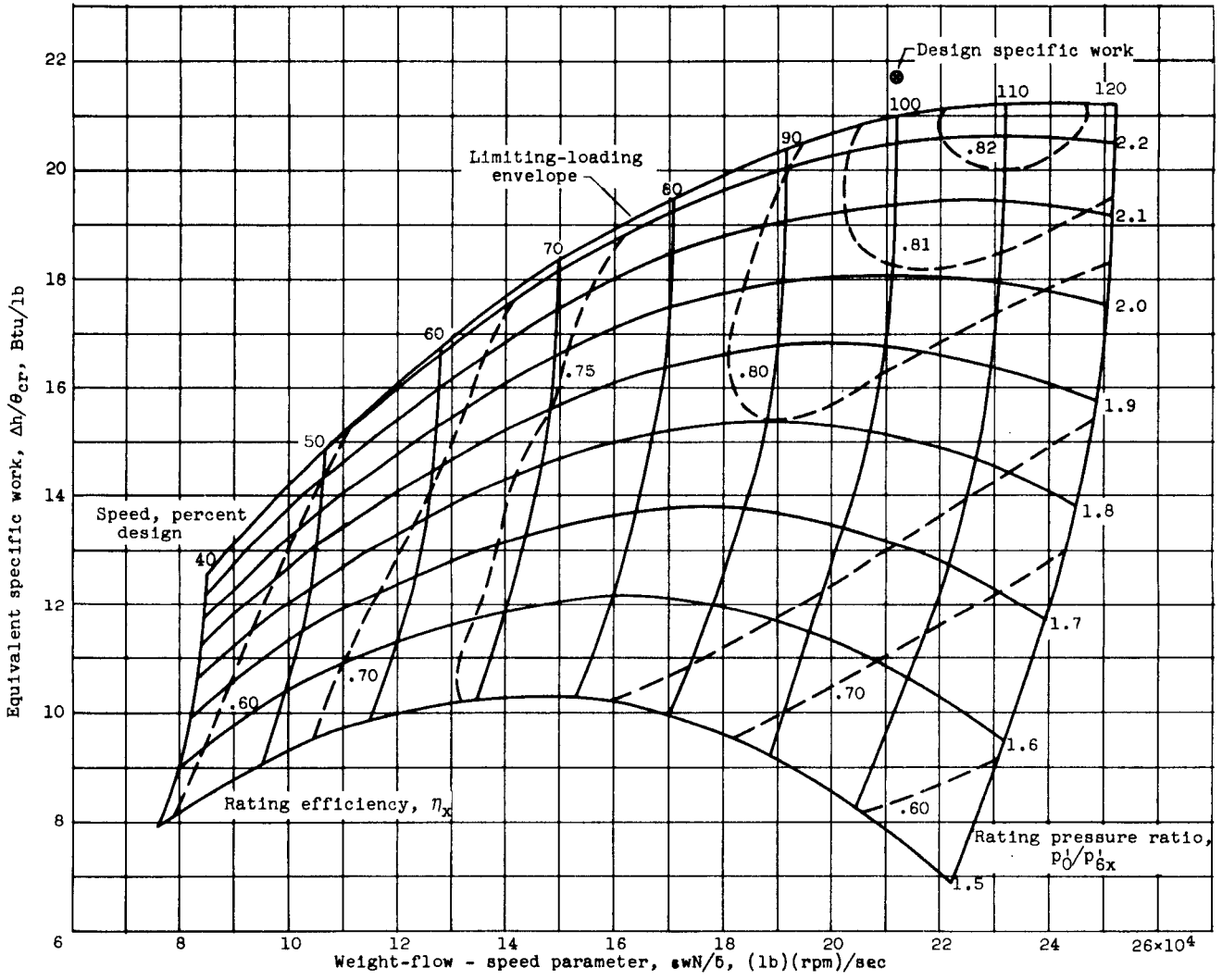

(b) Based on rating pressure ratio.

Figure 8. - Concluded. Over-all turbine performance with semivaneless stator.

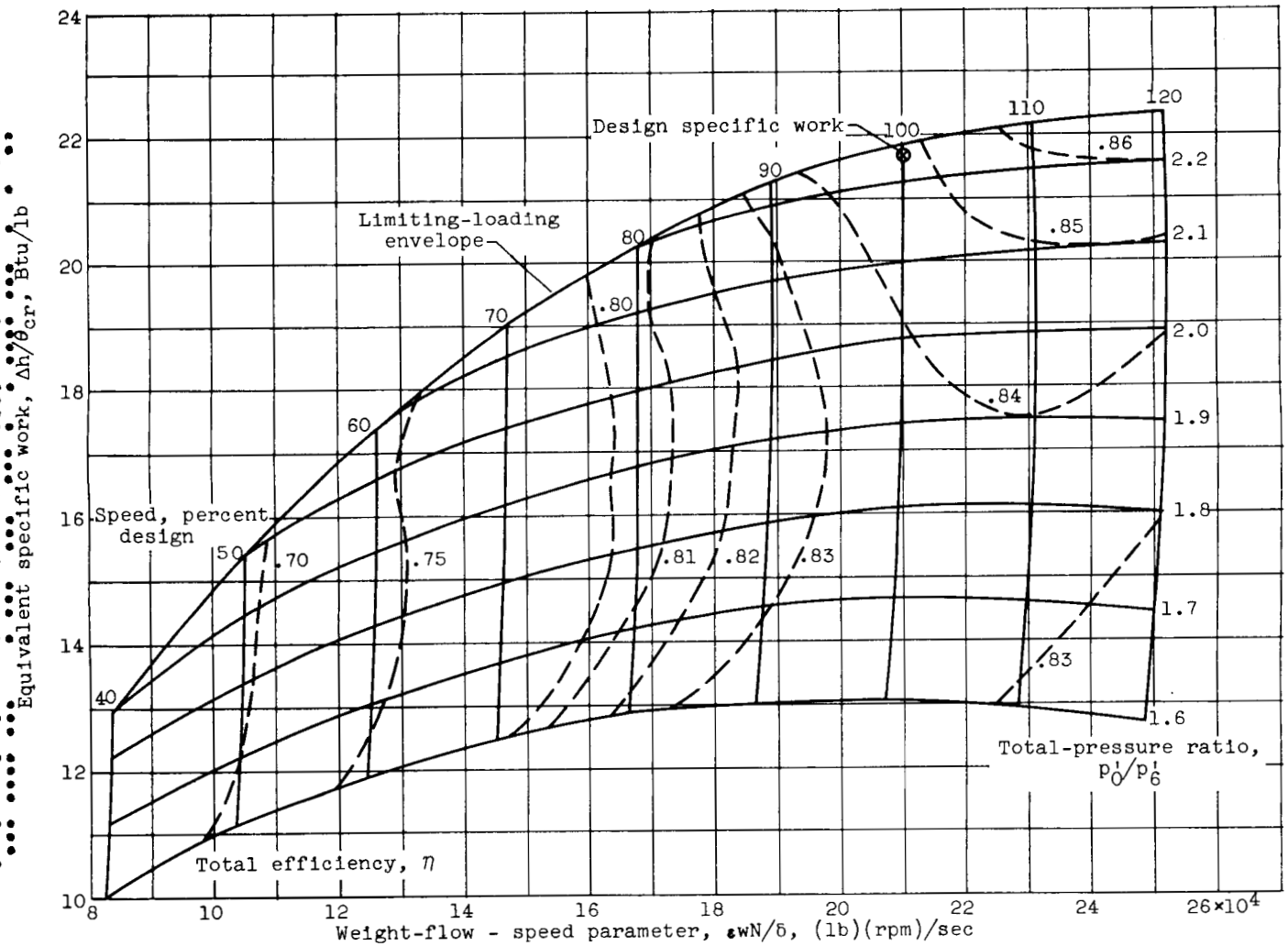

(a) Based on total-pressure ratio.

Figure 9. - Over-all turbine performance with standard stator with spacer.

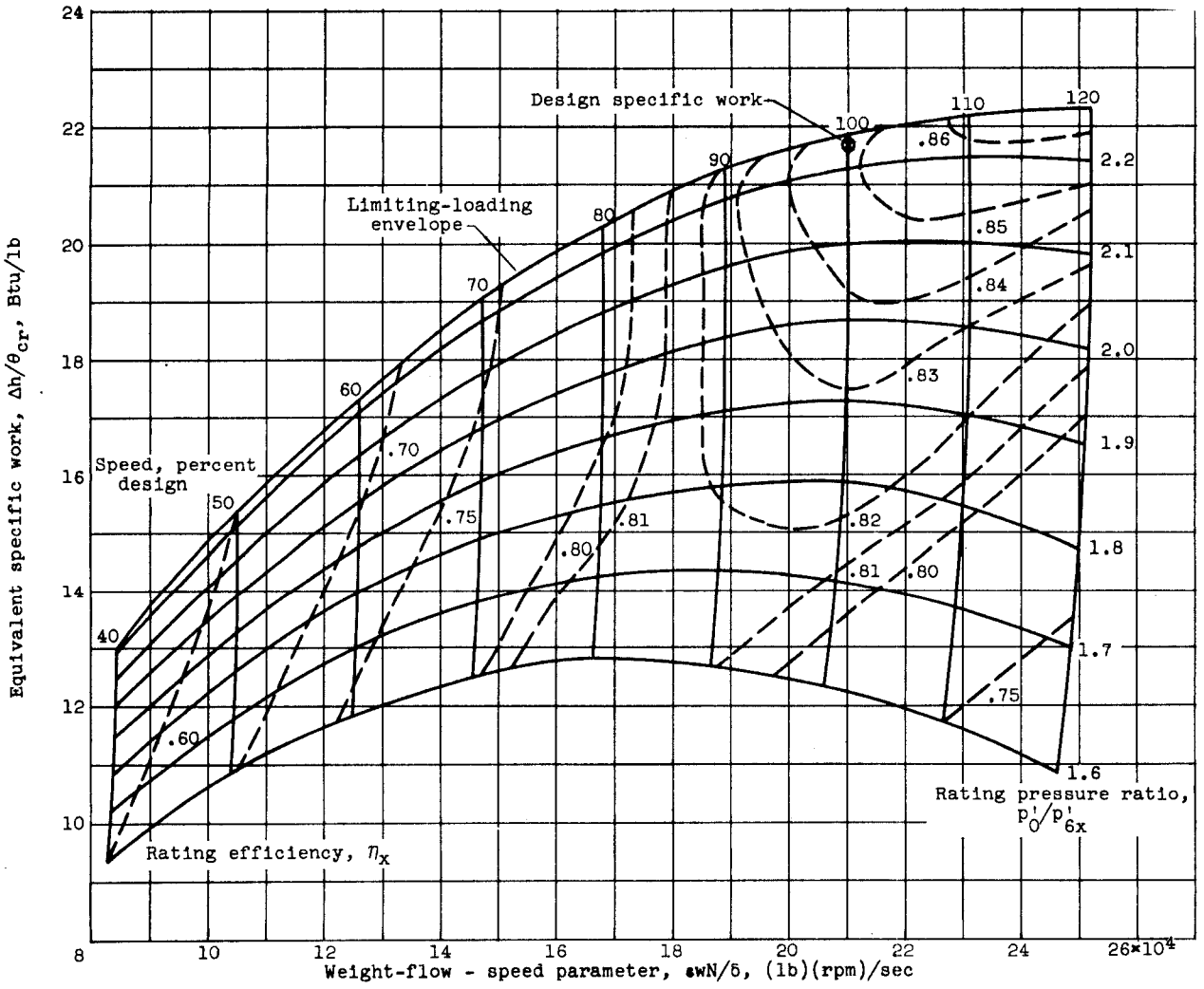

(b) Based on rating pressure ratio.

Figure 9. - Concluded. Over-all turbine performance with standard stator with spacer.

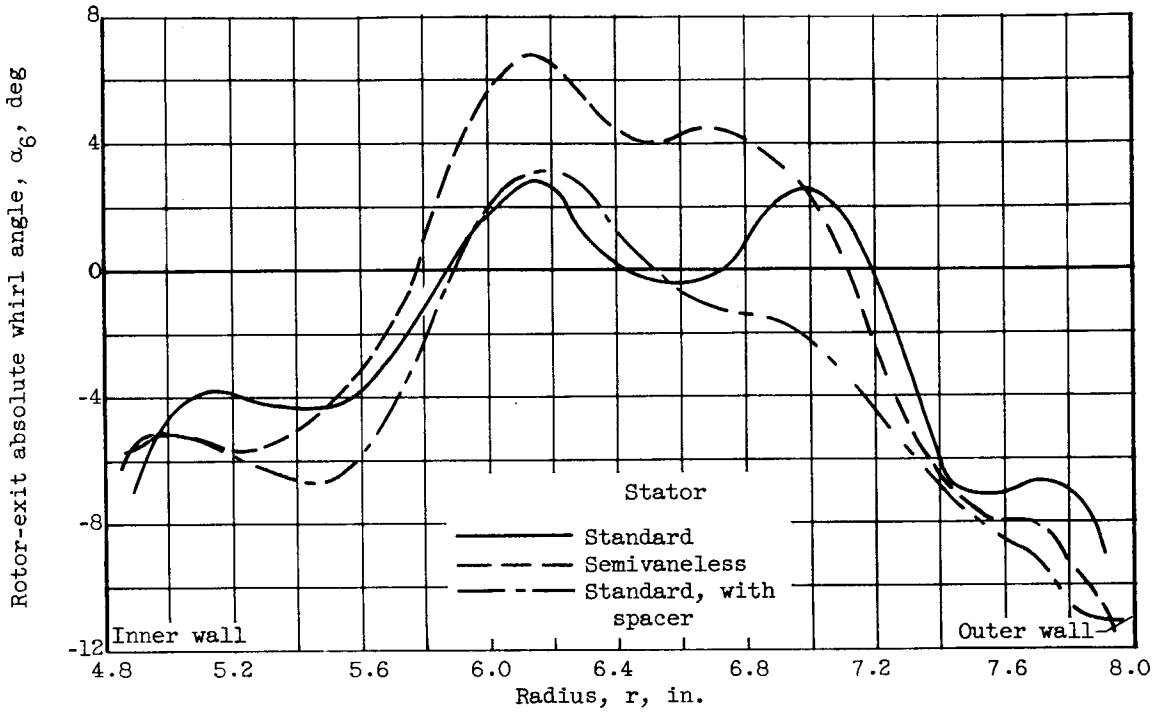

Figure 10. - Radial distribution of rotor-exit absolute whirl angle for turbine operating at design speed near limiting work.

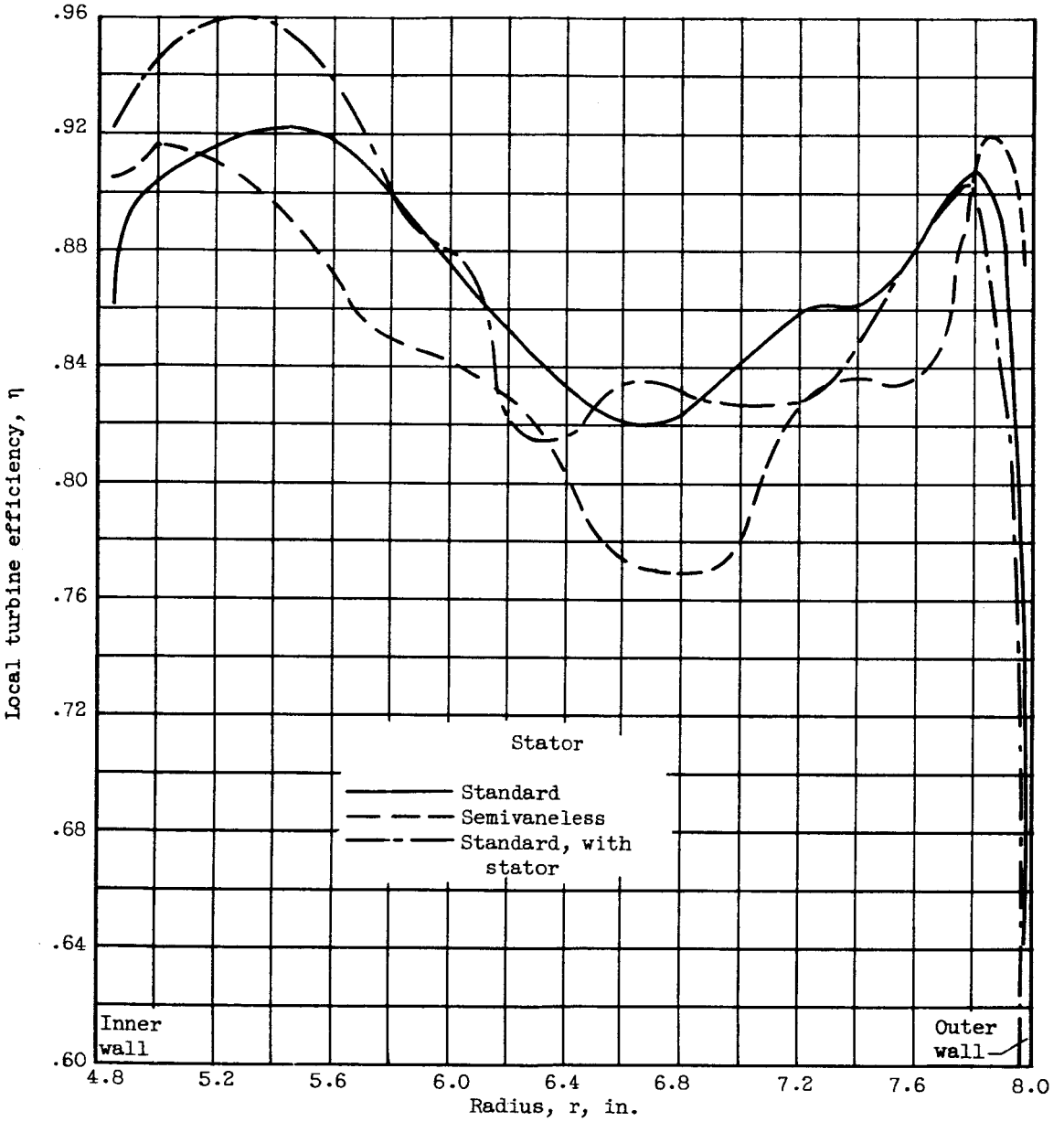

Figure 11. - Radial distribution of local efficiency from rotor-exit surveys made at design speed near design work.

CONFIDENTIAL